JAERI-M
6971

DIAGNOSTICS OF A SCRAPE-OFF LAYER PLASMA

March 1977

H. KIMURA, M. NAGAMI, S. YAMAMOTO, N. UEDA*,
H. OHTSUKA, H. MAEDA, and Y. SHIMOMURA

日 本 原 子 力 研 究 所
Japan Atomic Energy Research Institute

JAERI-M 6971

Diagnostics of a Scrape-off Layer Plasma

Haruyuki KIMURA, Masayuki NAGAMI, Shin YAMAMOTO, Noriaki UEDA*, Hideo OHTSUKA, Hikosuke MAEDA, and Yasuo SHIMOMURA

Division of Thermonuclear Fusion Research, Tokai, JAERI

(Received January 31, 1977)

The methods measuring a scrape-off layer plasma of DIVA (JFT-2a) are reviewed. In conclusion, these all should be effective in the next-generation devices with divertor.

---

* On leave from Mitsubishi Atomic Power Industry, Saitama, Japan

JAERI－M 6971

スクレープ・オフ層プラズマの計測

日本原子力研究所東海研究所核融合研究部

木村晴行・永見正幸・山本　新・上田憲照*
大塚英男・前田彦祐・下村安夫

（1977年1月31日受理）

DIVA（JFT－2a）のスクレープ・オフ層プラズマの計測に用いている種々の測定方法の総括を行い，併せてこれ等の測定方法が次世代の大型ダイバータ装置に於いても有効であることを示す。

* 三菱原子力工業株式会社

目　次　な　し

I. Introduction

Probes have been greatly contributing to plasma experiments because of their variety, simplicity, small size and easy scanning, but they seem unsuitable to be appplied to a high temperature and/or high density plasma especially a well confined plasma because of their disturbance to the plasma. Recently, they were tested to be applied to a tokamak plasma in DIVA, and it was observed that a small probe with a diameter of 0.25 mm immersed by a few mm's inside a separatrix magnetic surface induced a negative spike instability. In the scrape-off layer plasma, however, various kinds of probes were successfully applied without a serious disturbance. Probe measurements in DIVA evaluated plasma parameters, floating potential, space potential, charged particle flux, heat flux, diffusion coefficient, drift surface of runaway electrons, field configurations, fluctuations, deposited metal impurity on the neutralizer plate and also particle confinement time. These measurements in a scrape-off layer plasma in DIVA are reviewed in Section II.

The successful application of probe measurements in DIVA encourages us to discuss the possibility of probe measurements in a large device, which is discussed in Section III.

II. Probe Measurements in DIVA

The cross-sectional view of DIVA and typical plasma parameters are shown in Fig. 1. The detailed description of the device are given in ref. (1). A separatrix magnetic surface as a magnetic limiter is stably obtained inside material surfaces.[2] Probe measurements are applied to the scrape-off plasma. Probes are scanned mainly at R=40, 42, 44 and 68 cm and two dimensional scanning covering the whole cross-section of the scrape-off layer is also done.

2.1 Single and Double Langmuir Probes[3)4)]

Single and double Langmuir probes were used to measure electron temperature T_e, density n_e, floating potential V_f, space potential V_s, fluctuations and also diffusion coefficient. Three kinds of metal, i.e. Mo, Au and SUS 304L, were tested and the same probe characteristics and the same ion saturation currents were obtained by these three probes. Verious sizes (diameters of 1, 2 and 3 mm and length of 1, 2, 3 and 5 mm) were also tested and it was shown that the ion saturation current is proportional to the real

area of the probe surface not to that of the projected surface by the magnetic field line. Typical probe characteristics are shown in Fig. 2. The accuracy of determining electron temperature is dominantly affected by fluctuations discribed below and is typically 30 %. Typical ion saturation current profile are shown in Fig. 3. Diffusion coefficient is calculated from the ion saturation current profiles at different radii (see Fig. 4) and is $(3\text{-}1)\times10^3\ \alpha\ cm^2/sec$ where α is the ratio of the flow velocity along magnetic field lines to the ion sound velocity and is measured to be 0.2 - 0.5 (see 2.2). Then, the diffusion coefficient is about $10^3\ cm^2/sec$. The electron temperature is typically 25 eV - 5 eV and its profile is shown in Figs. 18 and 20.

A typical equi-floating potential surface and the maximum density surface are shown in Fig. 5 which shows the separatrix configuration in the divertor.

The movable protection plates, the movable shell and the shell are also used as single Langmuir probes and plasma particle loss from the main plasma are measured as ion saturation currents during only 20 μsec because of eliminating serious disturbance to the plasma. Current-voltage characteristics of the shell is shown in Fig. 6. The estimated particle loss rate is about 1.4 ms, which is consistent with the particle confinement time of 2 ms determined from the measurement of H_α line.

Fluctuations of ion saturation currents and floating potential are under investigation (see Fig. 7). These fluctuations, which have not been identified yet, presumably enhance the particle diffusion across magnetic field lines during the transit time of ions to the divertor along field lines and may be responsible for the relatively small value of the particle divertor efficiency.

2.2 Directional Probe[3)4)]

In order to measure the particle flux to the divertor, we use a pair of oneside parallel plane Langmuir probe, named a directional probe, which collects particles in opposite directions. Fig. 8 shows a sketch of the directional probe. Ion saturation current and electron saturation current patterns obtained by rotating the directional probe is shown in Fig. 9. The figure exhibits that plasma flows to the divertor along the magnetic field line and a cross field flow (e.g. ExB flow) are less than detectable. An undetectable cross field flow, however, has a possibility to affect the plasma flow because of the small value of the rotational transform ($B_R/B_T \leq 0.05$). The flow to the divertor is calculated from the difference between the upstream ion saturation current and the downstream. The flow velocity is also calculated assuming the shifted Maxwell distribution and typically $0.25\sqrt{T_e/M_i}$.

The flow velocity, however, is not constant along the vertical plane as shown in Fig. 10.

The accuracy of the particle flux determined by this method depends mainly on the accuracy of determining the flow direction. Assuming the flow direction coincide exactly to the magnetic field lines, the particle flux to the divertor is about ten times less than that to the shell surface and protection plate. From this result, the particle divertor efficiency is rather small and 10 % in this case.

2.3 Faraday Cup[4)]

Faraday cup, multigrid analyzer, was employed to measure ion temperature T_i and is schematically shown in Fig. 11. Ion temperature and drift velocity are calculated assuming the shifted Maxwell distribution from an obtained retarding curve. The typical example is shown in Fig. 12, and T_i = 25 eV which is consistent with the value obtained from Doppler broadening.

Electron temperature and ion saturation current are also obtained from the Faraday cup, even in the presence of high energy electrons.

2.4 Thermocouple Probe and Bolometer Probe[5)6)]

Measurements of heat flux were performed by a fine thermocouple covered by stainless steel with an outer diameter of 0.25 mm which is schematically shown in Fig. 13, and a bolometer of thin Ni-film is under investigation (see Fig. 14). The time constant of the thermocouple is 5 ms and the bolometer 0.2 ms (see Fig. 15). These probes are electrically connected to the vacuum chamber so as to simulate the same boundary conditions as the divertor plates with respect to the plasma flow in the scrape-off layer, however, the question whether the probe simulates the divertor plates or not is still left open because of the difference in the structural material.

The outputs of these probes are shown in Fig. 16. The heat flux measurements by the thermocouple are difficult because of a large noise when the grounded thermocouple probe is placed near the path of high energy electrons (see Fig. 16-c). To avoid these situations, time evolution of the heat flux near the path of high energy electrons is measured by decreasing the divertor hoop current to zero within about 200 μsec at a given time (see Fig. 18)[8)].

Profile of heat flux at R = 40 cm is shown in Fig. 20. Energy balance of the plasma is following:

Joule input ~60 kW

Convection and condition loss-40kW

(40% to divertor
60% to wall)

Radiation and CX loss ~20 kW

These results show that about 40 % of the energy loss by charged particles is guided into the divertor. This value is rather large comparing with the particle divertor efficiency. The relations between electron temperature, ion saturation current and heat flux are shown in Fig. 18, Fig. 19 and Fig. 20. These data show that the heat flux into the divertor is much larger than the value obtained from the plasma flow assuming a normal plasma sheath. In ref. (7), it is shown that this large heat deposition rate is due to the presence of high energy electrons.

2.5 X-ray Target

In order to investigate trajectories of runaway electrons in low density discharges, we used a small X-ray target. The target is a piece of Molybdenum of cylindrical shape (4 mm diameter) and its axis is parallel with the toroidal magnetic field. One side of the cylinder is cut-off under the angle 45° and this aurface is the source of X-ray radiation which we observed. The target is originated so that the runaway electrons form the main plasma can hit the observed surface. The collimation is so made that the X-ray beams from that surface can pass to the NaI scintillator and the light from the scintillator is transmitted to the photomultiplier, using fiber light guides. In order to fix the view angle of the scintillator, the target, the scintillator and the collimator are set into one probe which can be scanned vertically.

X-ray energy which we observe with 100 % efficiency ranges from approximately 10 keV to 100 keV determined by the thickness of Aluminum window and the hight of an NaI scintillator.

Fig. 21 shows the X-ray signals from a target placed at $z = 4.0$, 3.25 and 3.0 cm when the divertor hoop currents reduced at 15 ms. It was shown that the path of the runaway electrons moves according to shrinking of the separatrix magnetic surface in the divertor region.

A large target of 15 mmϕ and the protection plates are also used as X-ray targets (see Fig. 22).

Comparing the observed runaway drift surfaces and the calculated results, we can obtain a fine structure of the field configuration near the separatrix magnetic surface.

2.6 Other Probes

Conventional small magnetic probes with the case diameter of 3 mm are also employed and a metallic impurity collector will also be used. The metallic impurity is a metallic stick which will be exposed in the scrape-off layer plasma during several hundreds of discharges. After exposing the probe, the surface contamination will be investigated. Figure 23 shows the Au profile on the neutralizer plate exposed during an early phase of DIVA experiment.

2.7 Summary

Various kinds of probe measurements are successfully applied to investigate the scrape-off layer plasma in DIVA. These measurements evaluated plasma parameters, floating potential, space potential, charged particle fluxes to the wall and to the divertor, heat flux, diffusion coefficient, drift surfaces of runaway electrons, field configurations, fluctuations, deposited metallic impurities on the neutralizer plate and even the particle confinement time.

III. Discussion of Probe Measurements in a Large Device

In a future large device, probe measurements do not seem suitable because of its large heat flux, a high temperature and/or high density plasma even in a scrape-off layer. The scrape-off layer plasma, however, contacts naturally to the structural material of the neutralizer plate and is largely affected by this material surface. Then, it seems reasonable to consider that the scrape-off layer plasma is not affected by a small additional material surface, i.e. a probe surface when the probe surface is carefully kept at good conditions (e.g. the same conditions as those of the neutralizer surface). In this section, some discussion about surface conditions are described.

The surface conditions exposing to a plasma are concerned with particle emission and scattering such as out gas evaporation, sputtering, reflection, sticking and secondary electron emission, and these phenomena depend on the following conditions.

(1) Surface Material and Surface Structure.
(2) Electrical Condition.
(3) Thermal Condition.

In the following subsections, these conditions are discussed.

3.1 Surface Material and Surface Structure

When the structural material of the probe surfaces is made of the same material as the neutralizer plate and is exposed to a plasma, there is no effect from the probe surfaces except the effect of moving a small surface from the neutralizer plate. When the material of the probe is different from the neutralizer plate, the effects of the probe surface should be carefully discussed but the small size of the probe may reduce the disturbance down to the allowable level.

3.2 Electrical Condition

There is no problem in the electrical condition when the probe is electrically connected to the neutralizer plate. Therefore, only an electrostatic probe has problems because of applying a voltage between the probe and the neutralizer plate. It depends on plasma parameters especially on the electron and ion temperature whether the electrostatic probe measurements are available or not, and an electrostatic measurement seems impossible in a scrape-off layer plasma expected in PDX.

By the way, in order to reduce impurity contamination largely in a divertor device, it seems necessary to have a shielding divertor. The high temperature shielding divertor seems unsuitable because the scrape-off layer plasma sputters metallic impurities from the neutralizer plate which are fully ionized and are easily built up by the self sputtering. For this reason, the low temperature shielding divertor, whose temperature is about 20 eV (threshould energy of sputtering yield by heavy atoms), is suitable and an electrostatic measurement is useful in this scrape-off layer.

3.3 Thermal Condition

Surface temperature is given approximately by the following equation, because it is very difficult to cool the surface during the discharge (e.g. the heat conduction length of Ti is 3 mm during 1 sec).

$$T_S = T_O + \Delta T \quad , \quad \Delta T = \frac{q\sqrt{\tau}}{\sqrt{\rho c \lambda}}$$

where T_O : base temperature

ΔT : rising temperature during exposing the surface to the plasma

q : heat flux density

ρ : density

c : heat capacity

λ : thermal conductivity

τ : exposing time

T_o can be kept near to room temperature by cooling the surface during the repetition time. On the neutralizer plate, τ is a current duration time τ_j. In order to avoid the effect of the probe surface, it is necessary to keep the surface temperature T_p of the probe lower than that T_N of the neutralizer plate. Therefore, the following equation should be satisfied.

$$\frac{\tau_P}{\tau_j} \leq \left(\frac{q_P}{q_N}\right)^{-2} \frac{\rho_P c_P \lambda_P}{\rho_N c_N \lambda_N} \sim \left(\frac{B_P}{B_T}\right)^2 \frac{\rho_P c_P \lambda_P}{\rho_N c_N \lambda_N}$$

where P indicates the probe surface and N indicates the neutralizer plate, and B_T and B_P are troidal field and poloidal field, respectively. In a typical case of $\rho_P c_P \lambda_P = \rho_N c_N \lambda_N$, $B_P/B_T = 1/7$ and $\tau_j = 1$ sec, $\tau_P \leq 20$ msec. It is not difficult to expose a probe only during 20 ms by scanning the probe or the magnetic field line.

In PDX, the maximum energy flux to the divertor is 4 MW and heat flux density on the probe surface is 3.5 kW/cm^2 assuming thickness of the layer = 1 cm and $B_P/B_T = 1/7$. This value is nearly equal to the maximum heat flux of 4 kW/cm^2 observed in DIVA in which the discharge duration is 30 ms.

3.4 Summary

Using a structural material of a neutralizer plate as a probe surface and scanning the probe or the magnetic field lines, all probes except an electrostatic probe can be applied in a scrape-off layer in a large device without a large disturbance to a plasma.

Acknowledgements

Our particular thanks are due to the JFT-2a Operation Group for their help. We should also like to express our gratitude to Dr. M. Tanaka for useful discussions.

References

1) SHIMOMURA, Y., et al., JAPAN ATOMIC ENERGY RESEARCH INSTITUTE REPORT, JAERI-M 6102 (1975).

2) SHIMOMURA, Y., et al., Proc. 7th Europ. Conf. on Controlled Fusion and Plasma Physics, Lausanne, 2 (1975) 81.

MAEDA, H., et al., Nuclear Fusion 16 (1976) 148.
SHIMOMURA, Y., et al., Phys. Fluids 19 (1976) 1635.

3) OHTSUKA, H., et al., submitted to Plasma Physics.
4) KIMURA, H., et al., JAPAN ATOMIC ENERGY RESEARCH INSTITUTE REPORT, JAERI-M 6861 (1977).
5) MAEDA, H., et al., to be published in Nuclear Fusion.
6) UEDA, N., et al., JAPAN ATOMIC ENERGY RESEARCH INSTITUTE REPORT, JAERI-M 6723 (1976).
7) MAEDA, H., et al., Proc. Int. Symp. on Plasma Wall Interaction, Jülich, Germany (1976).
8) SHIMOMURA, Y., et al., Nuclear Fusion 16 (1976) 587.

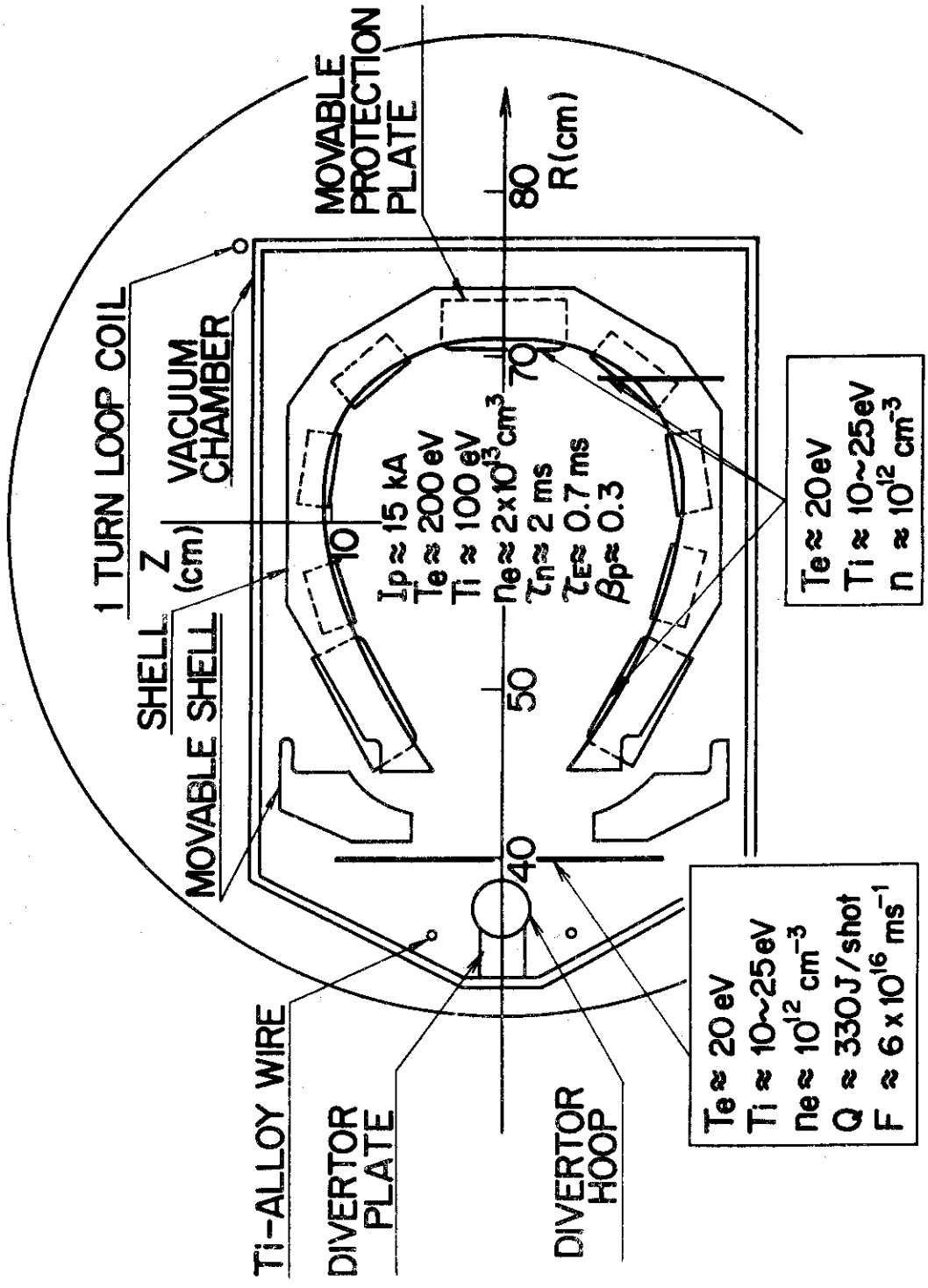

Fig. 1 Cross-sectional view of DIVA and typical plasma parameters

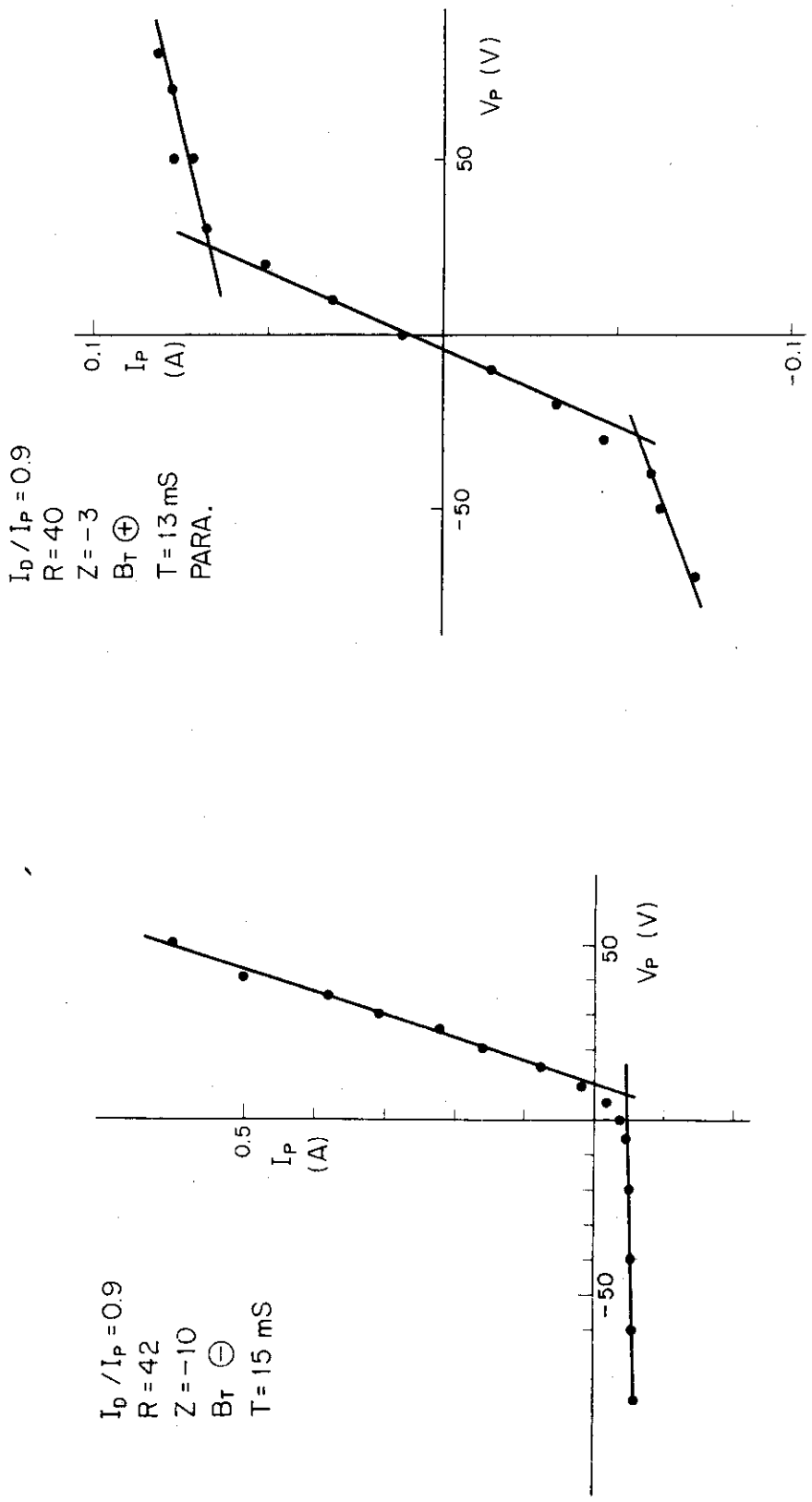

(a) by a single Langmuir probe

(b) by a double probe

Fig. 2 Probe characteristics in the divertor region of DIVA

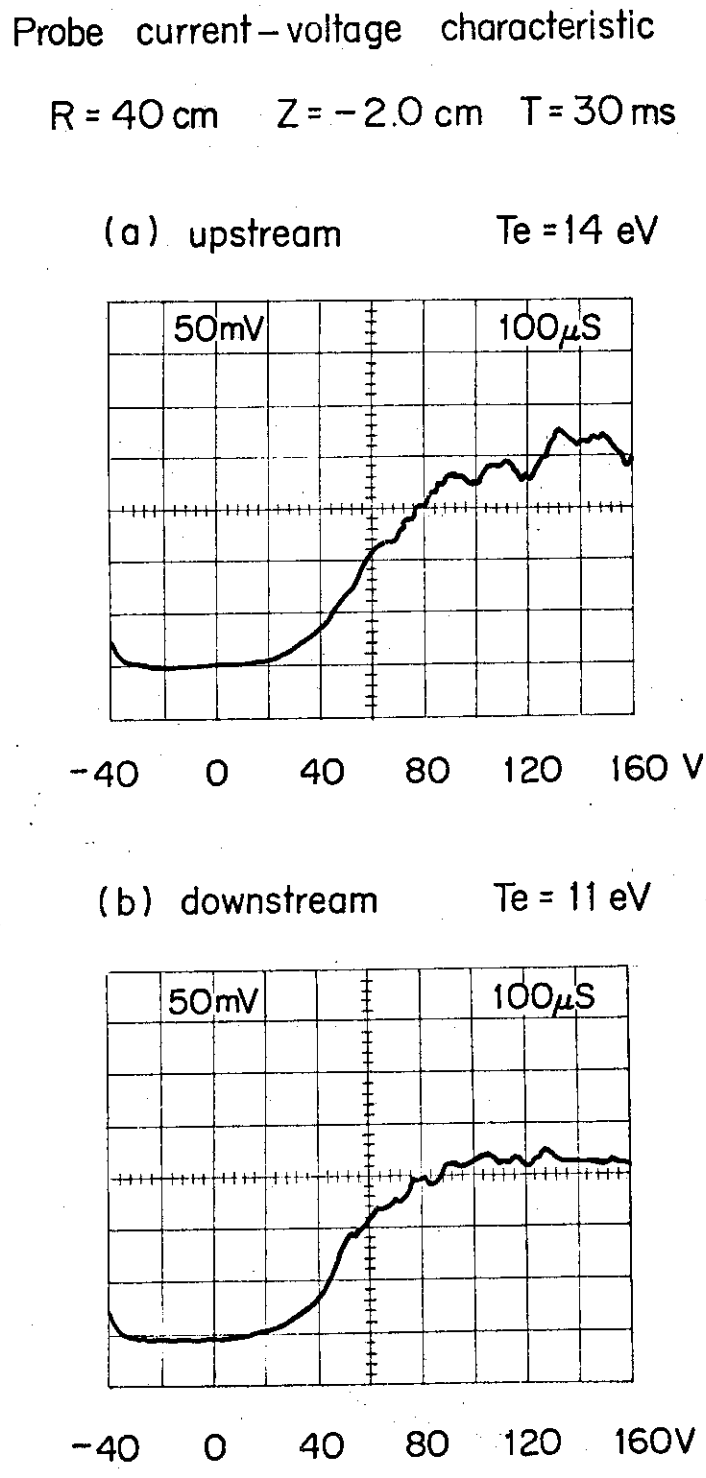

(c) by a directional probe (cf. 2.2)

Fig. 2 Probe characteristics in the divertor region of DIVA

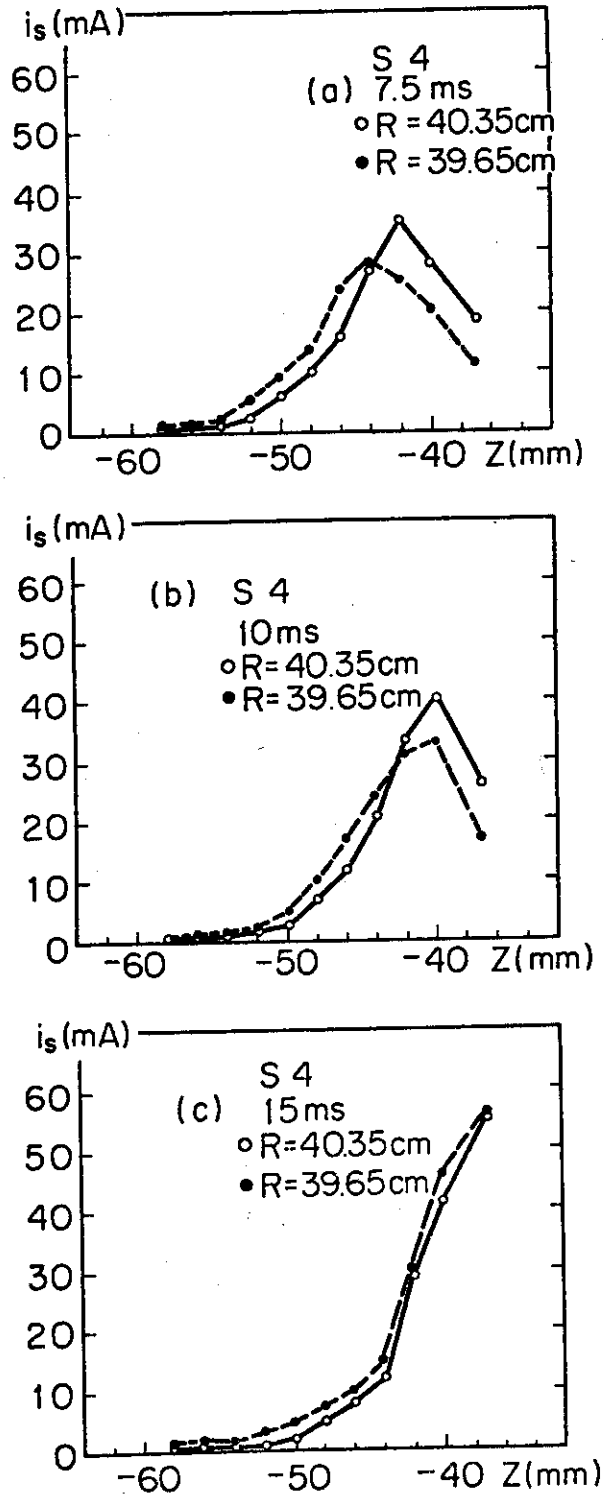

Fig. 3 Z-profiles of ion saturation current in the scrape-off layer of DIVA

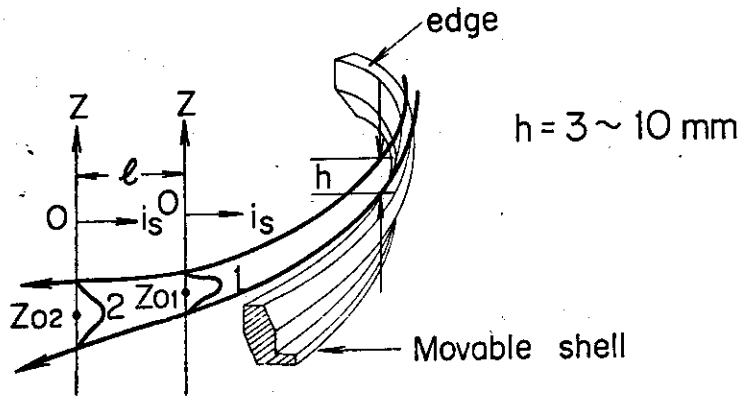

Fig. 4 Conceptional diagram of the measurement of a particle diffusion coefficient in the scrape-off layer of DIVA

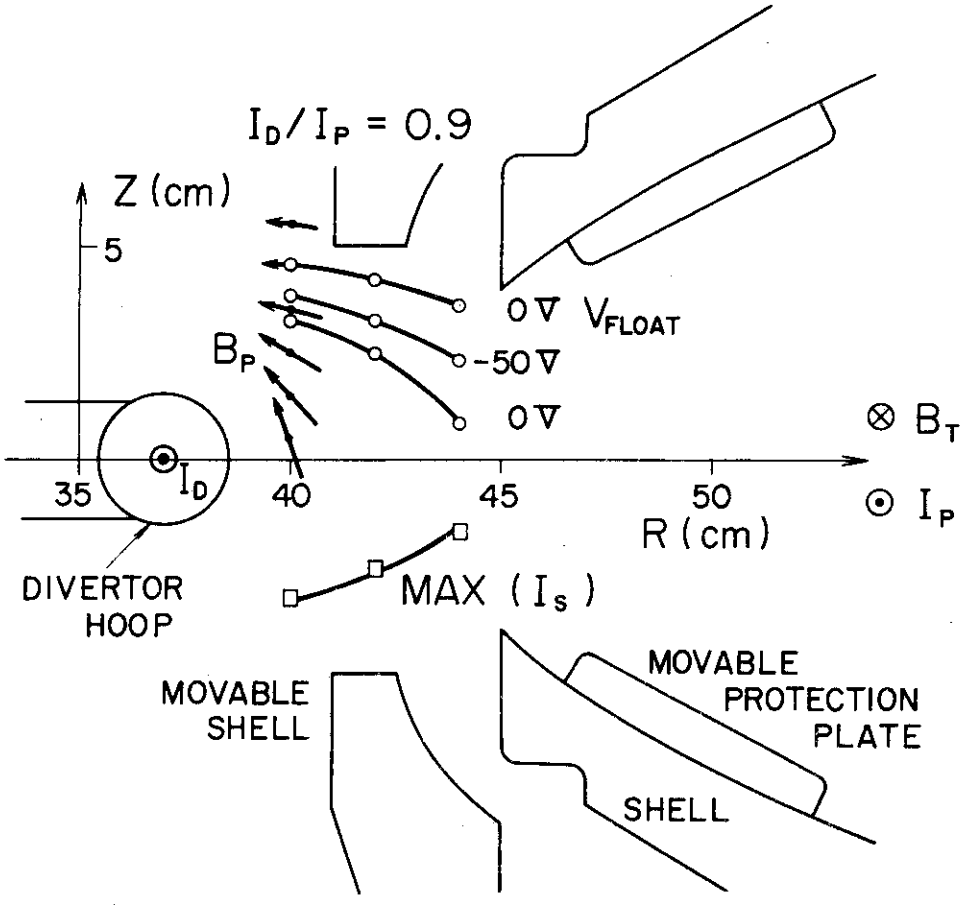

Fig. 5 Equi-floating potential and the maximum density surfaces

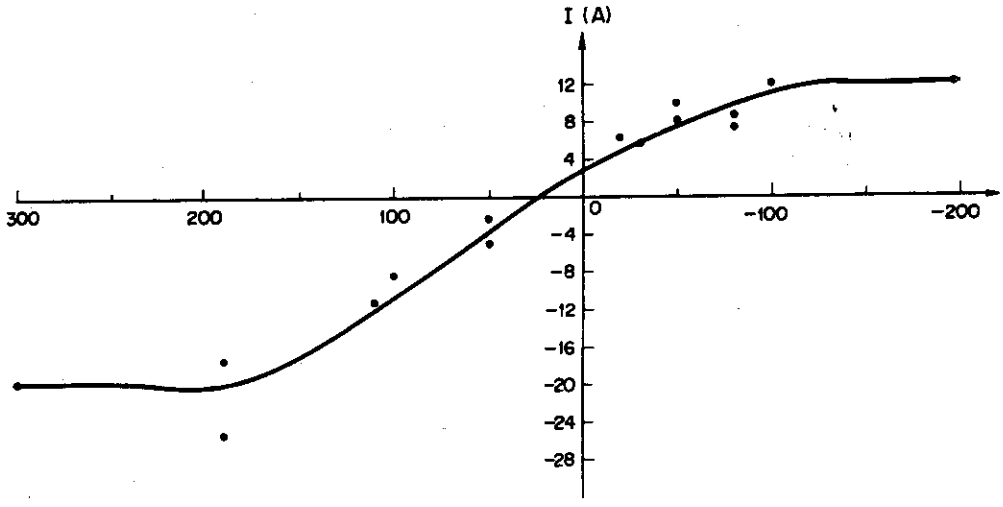

Fig. 6 Current-voltage characteristic of the shell, at 30 ms. The shell is biased with respect to the vacuum chamber

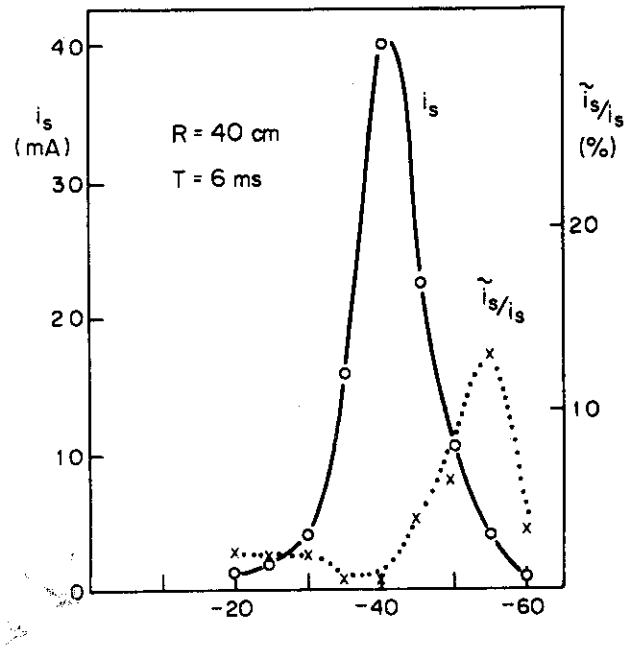

Fig. 7 Ion saturation current profile and its fluctuation profile

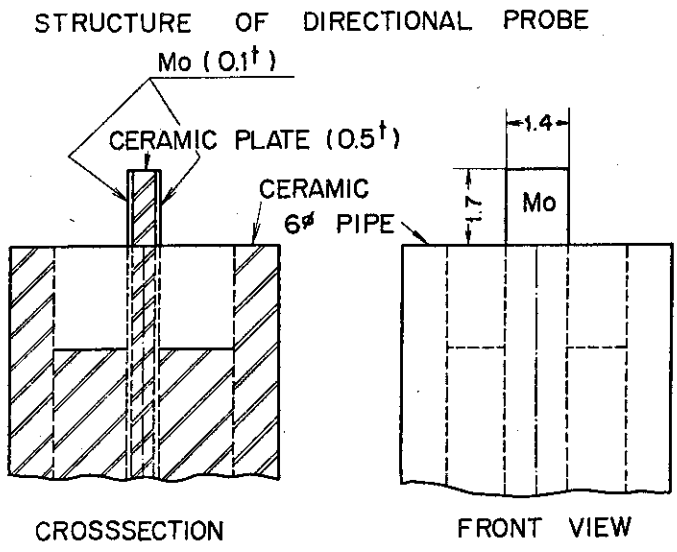

Fig. 8 Schematic drawing of a directional probe

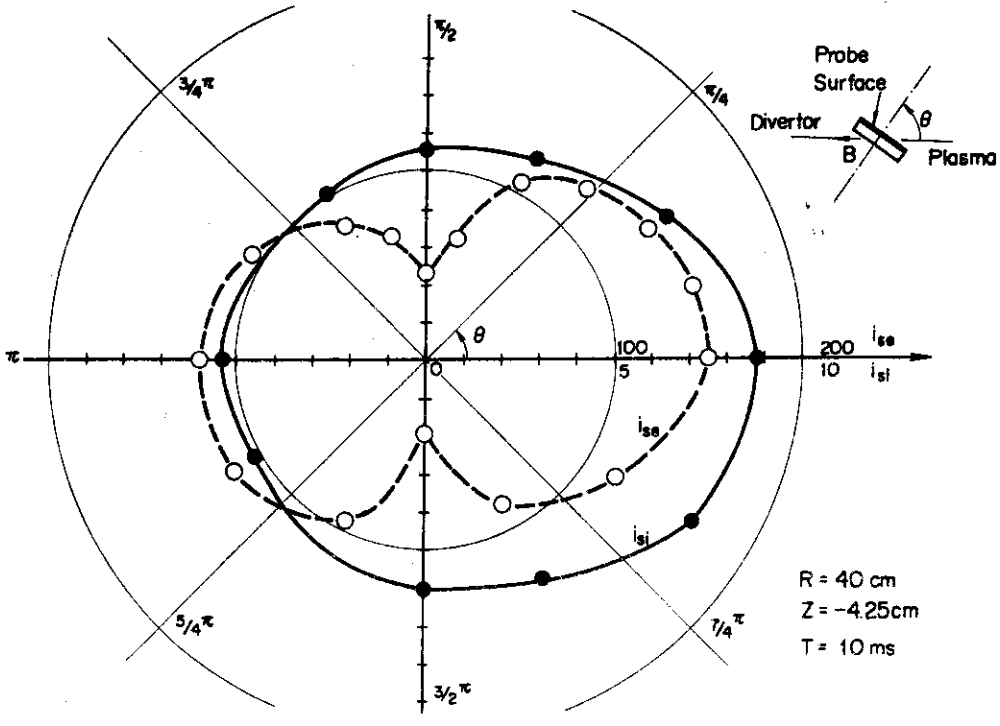

Fig. 9 Angular distributions of ion and electron saturation currents

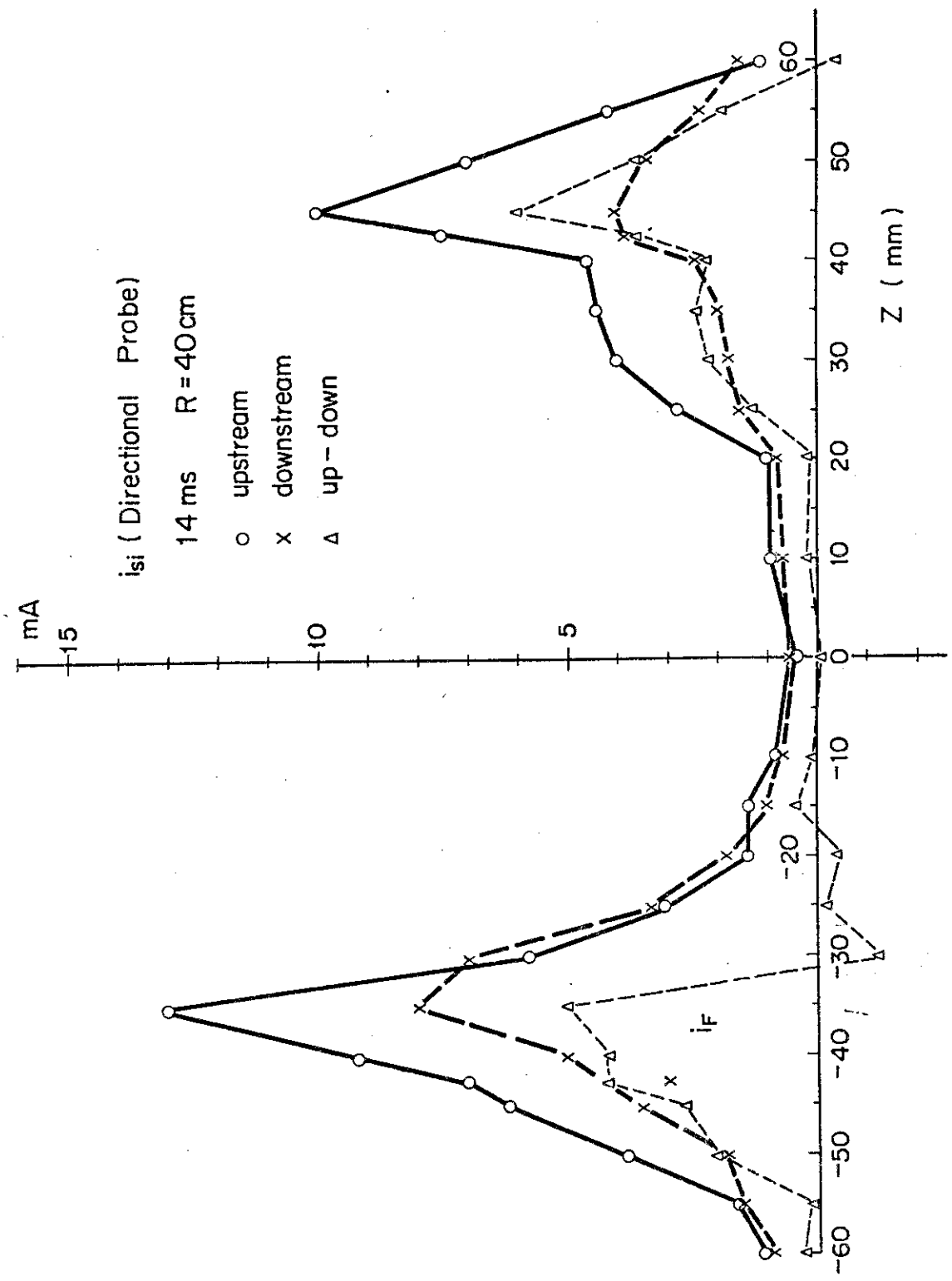

Fig. 10 Z-profiles of ion saturation currents in the divertor region of DIVA. Upstream means the plasma flow from the main plasma region to the divertor along the field line. Downstream means the one from the divertor to the main plasma region along the field line

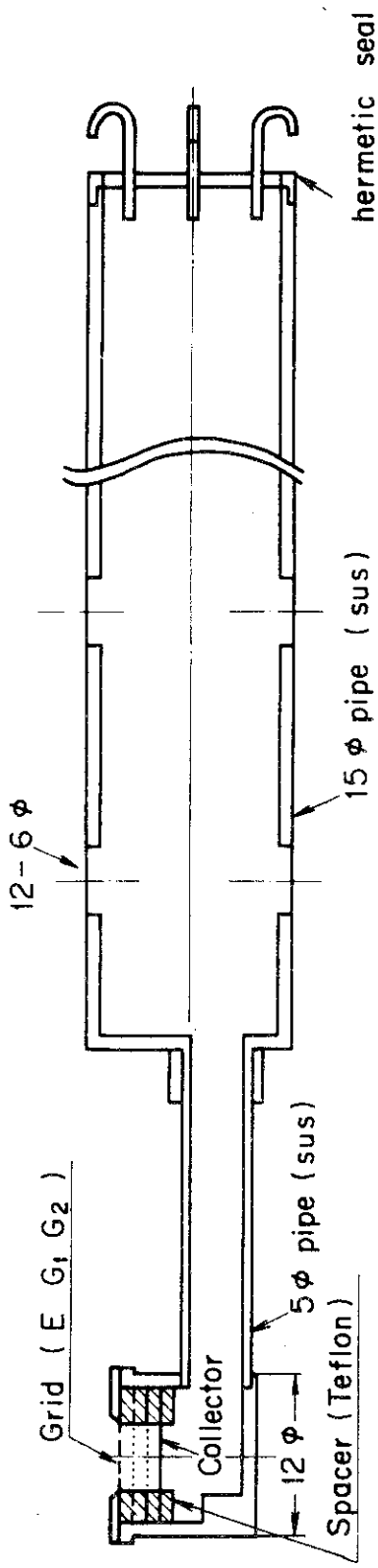

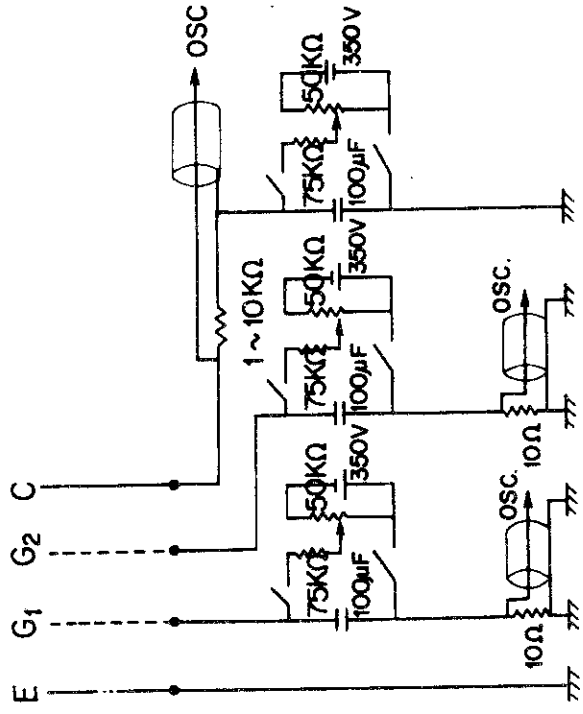

Fig. 11 Schematic drawing of a Faraday cup and its circuit

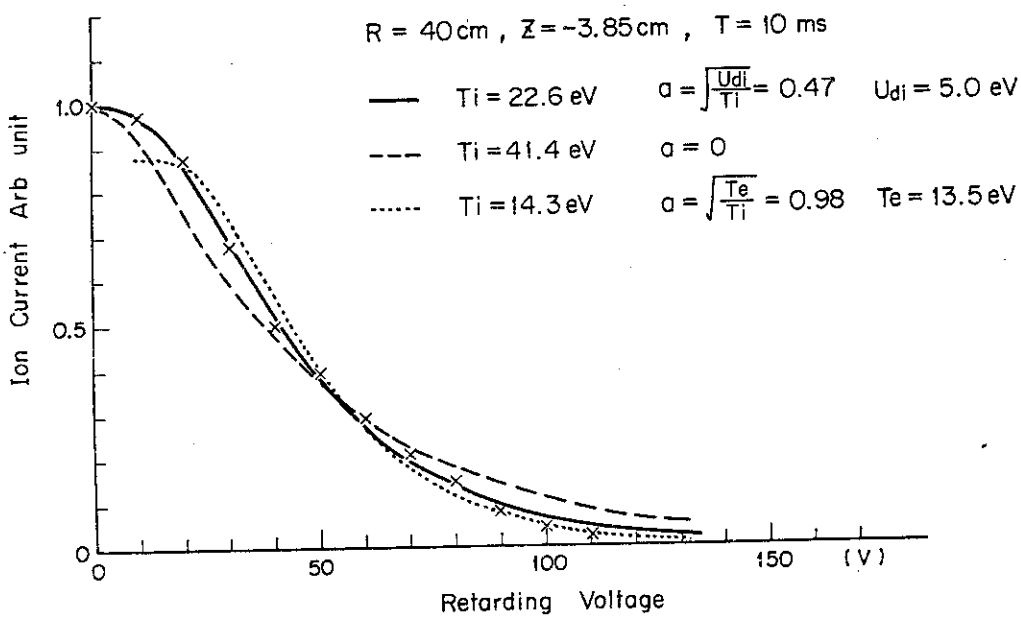

Fig. 12 Ion retardation characteristics from a Faraday cup

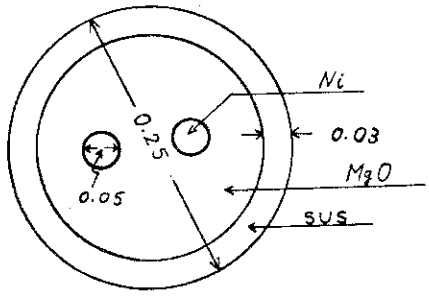

Material	S (cm²)	ρ (gr/cm³)	C (cal/gr°C)	SρC
S U S	0.0207×10^{-2}	7.9	0.115	1.84×10^{-4}
Ni	3.93×10^{-5}	8.9	0.115	0.40×10^{-4}
MgO	2.45×10^{-4}	3.6	0.29	2.56×10^{-4}
Sum				4.84×10^{-4}
ρC				0.99

Fig. 13 Fine thermocouple

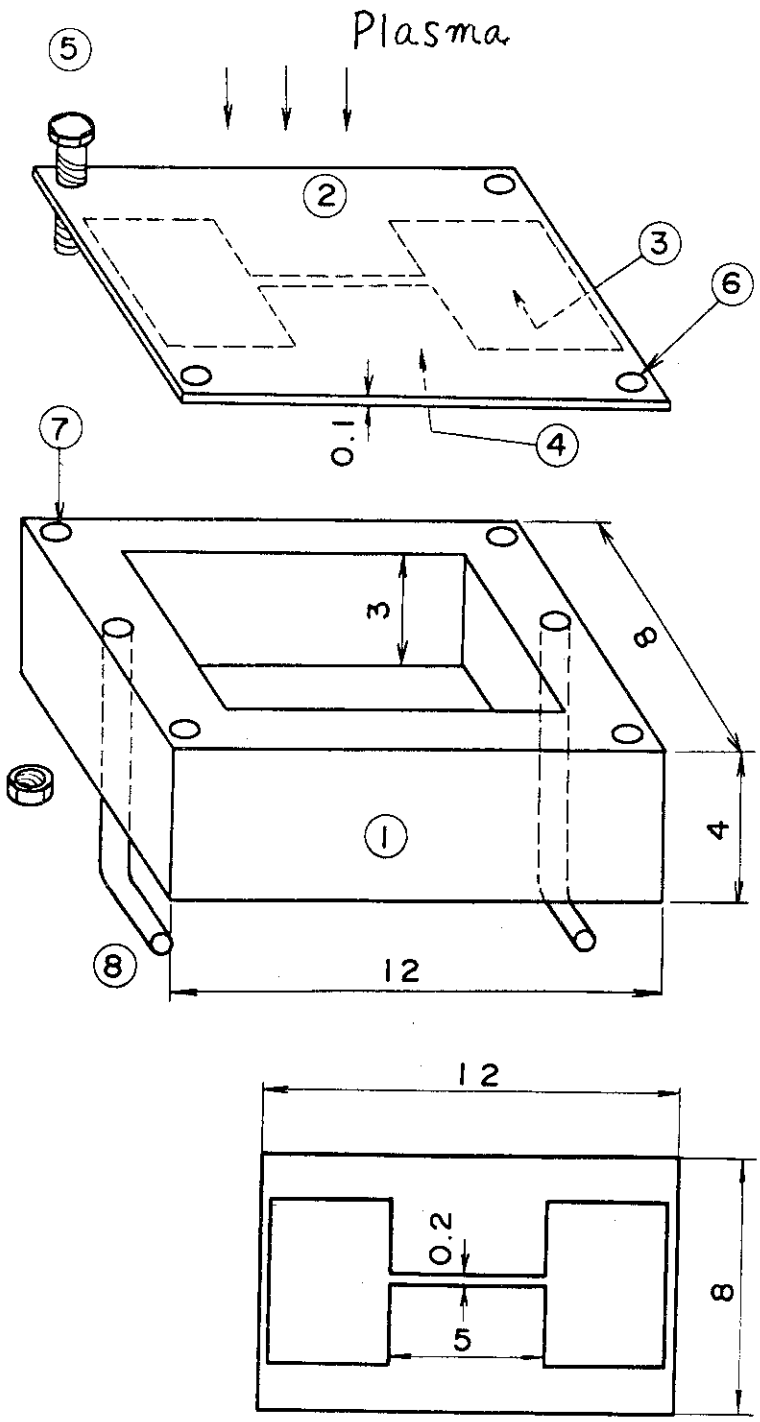

(1) Ceramic
(2) Mo
(3) Ni-film Resistance
(4) Si O Insulator
(5) Bolt
(6) 1 mm
(7) 1.5 mm
(8) Electrode

Fig. 14 Bolometer

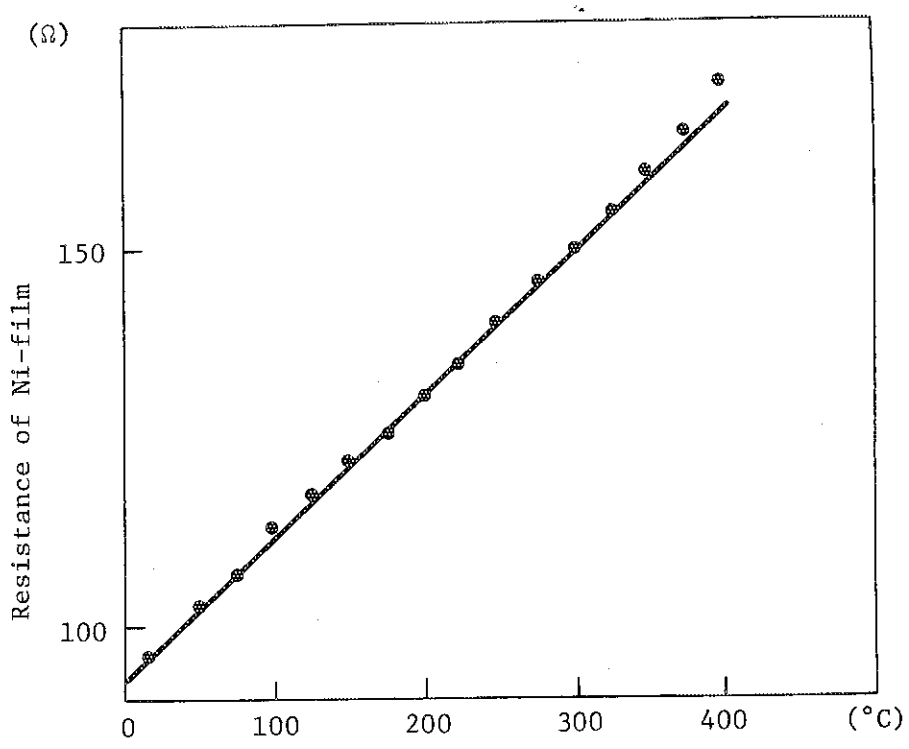

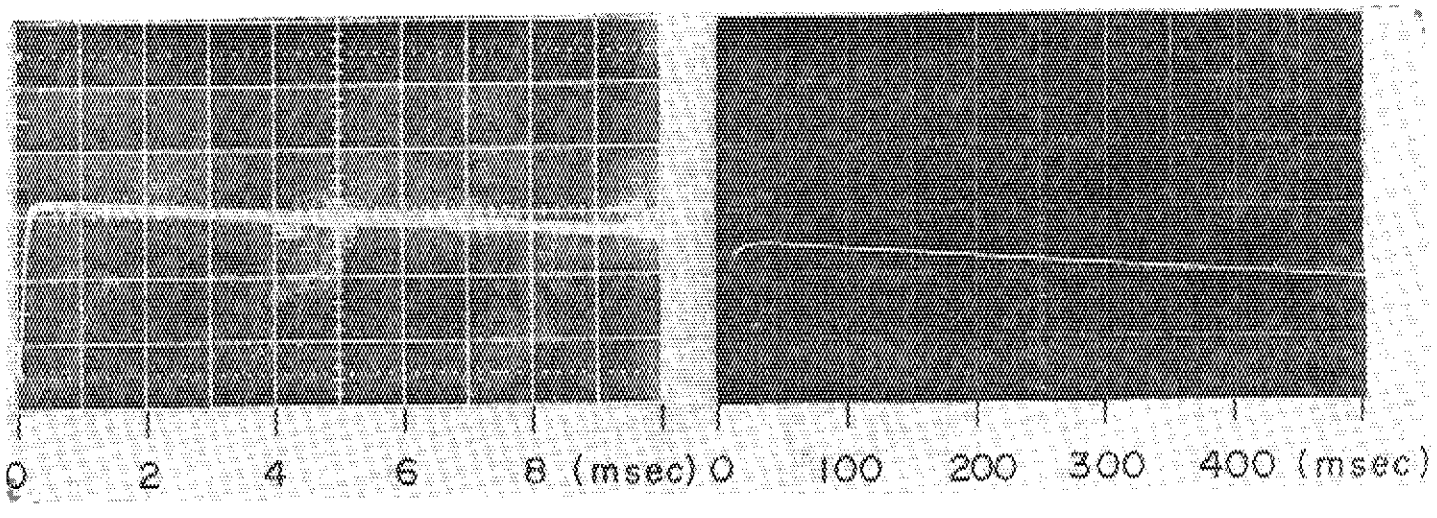

Ni-film Bolometer

Fine Thermocouple

Fig. 15 Characteristics of fine thermocouple and bolometer

Z = 40 mm

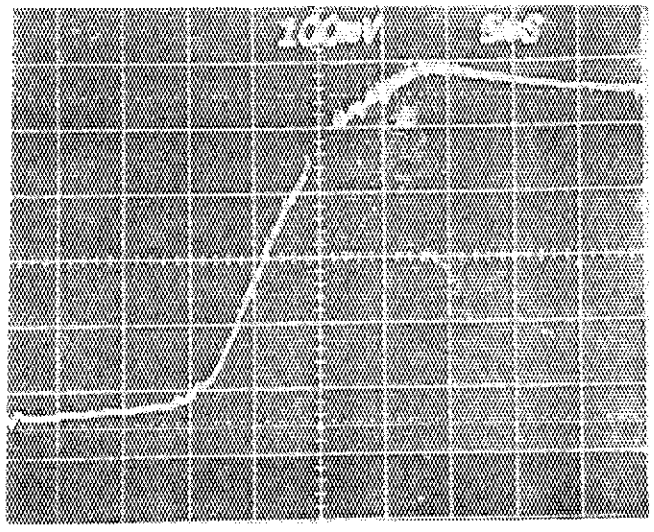

(a) Ni-film Bolometer

Z = 40 mm

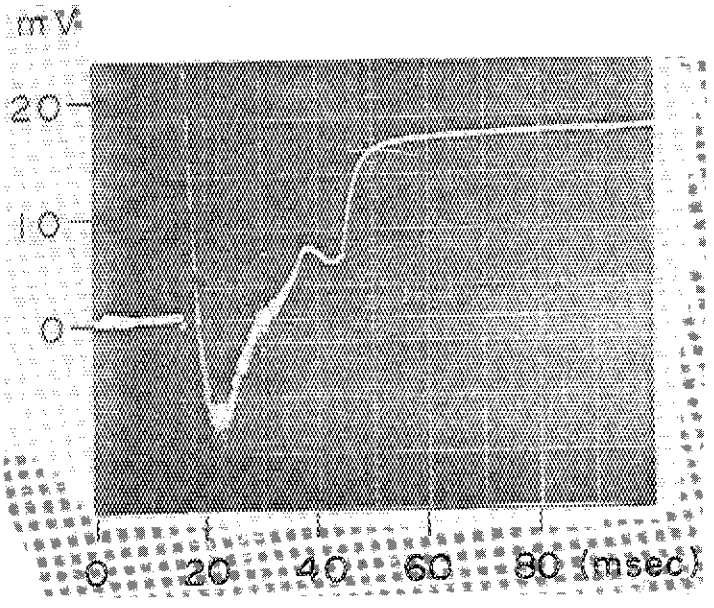

(c) Fine thermocouple

Z = -40 mm

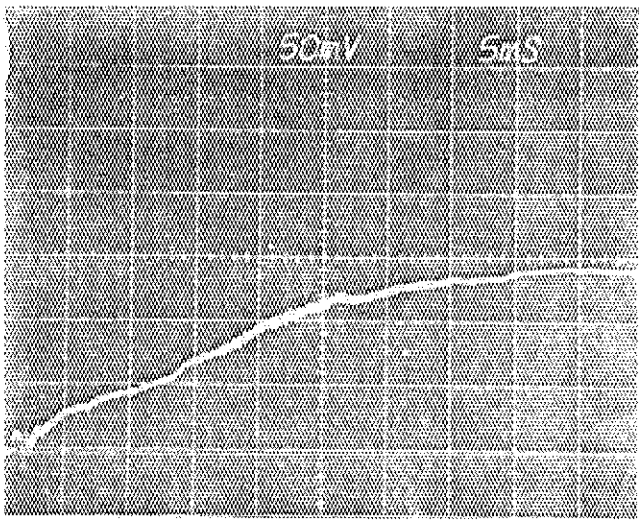

(b) Ni-film Bolometer

Z = -40 mm

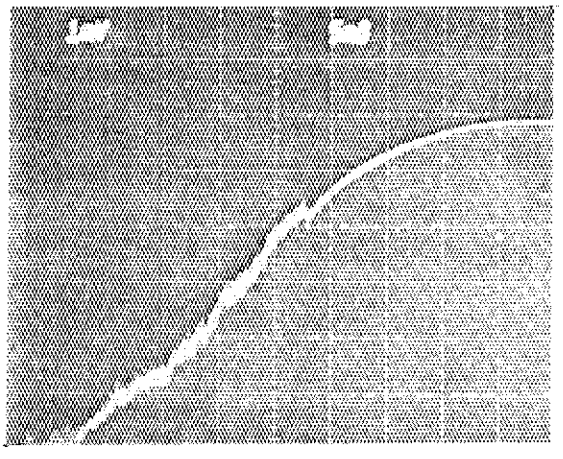

(d) Fine thermocouple

Fig. 16 Outputs of thermocouple and bolometer

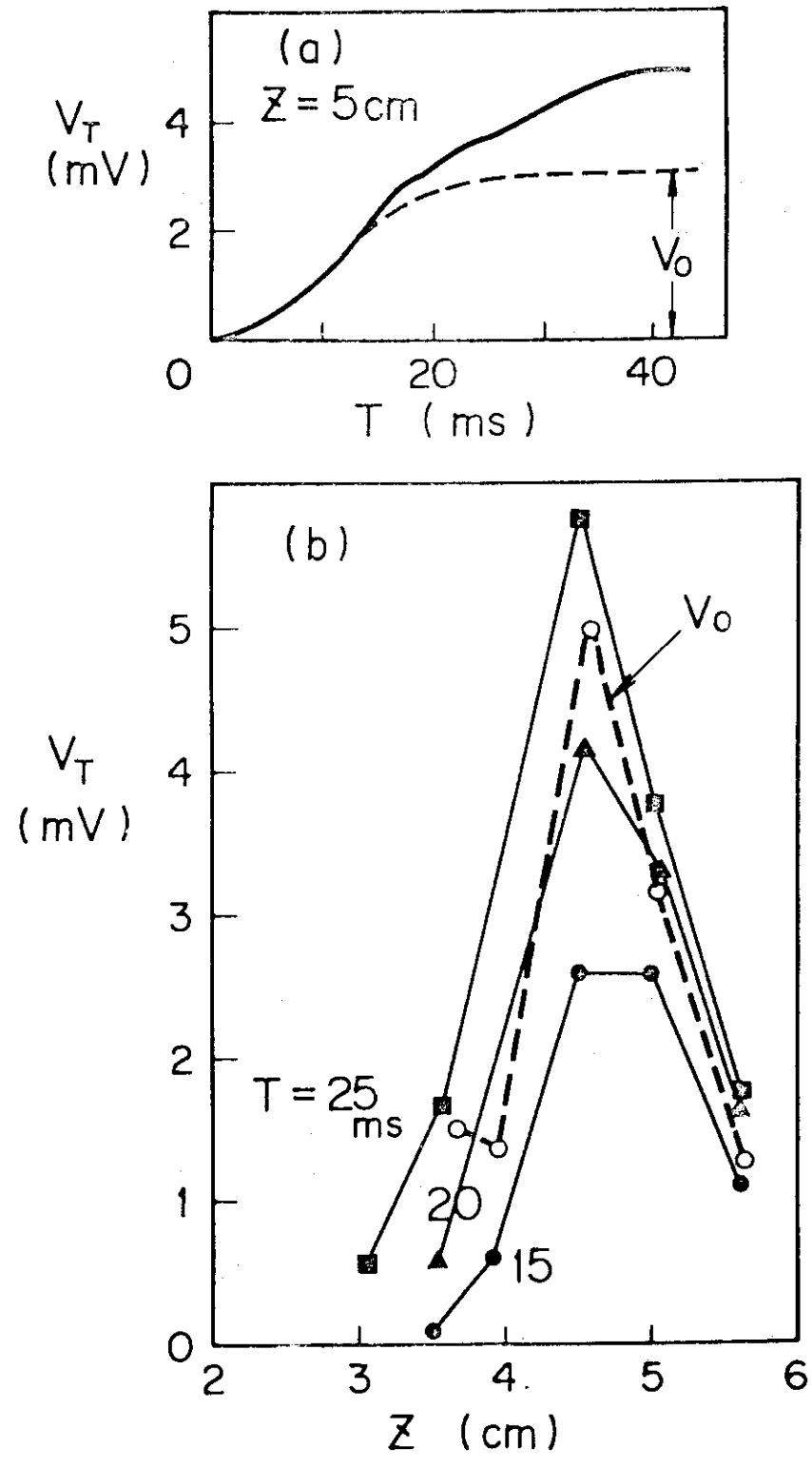

Fig. 17 Oscillograms of output of a thermocouple and profiles of the output in the divertor region. Solid lines correspond to the case of keeping I_D/I_P constant and dotted lines decreasing I_D/I_P down to zero at 15 ms

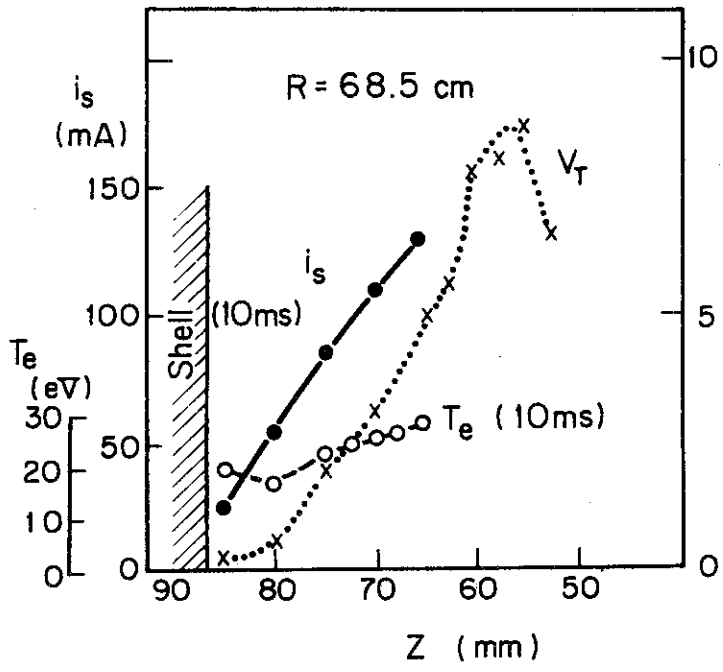

Fig. 18 Plasma profiles near the main plasma column

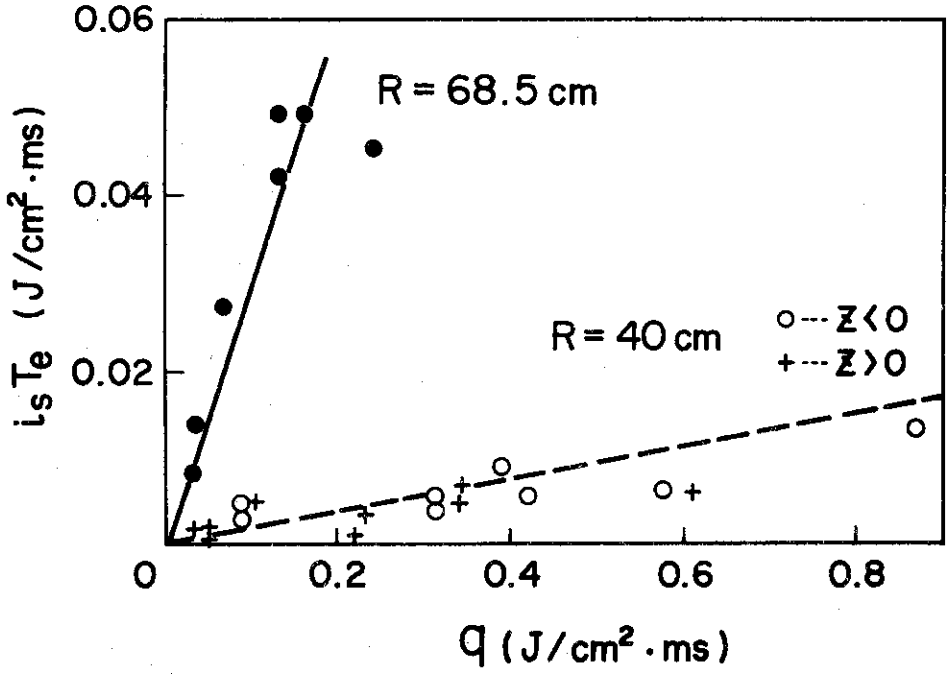

Fig. 19 Heat flux q and $i_s \times T_e$ in the divertor and near the main plasma column

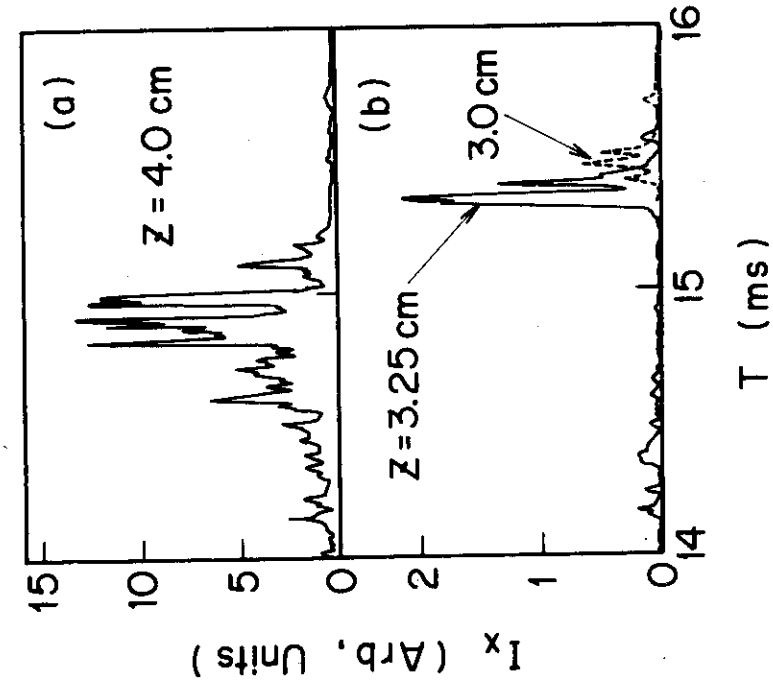

Fig. 21 X-ray from a target when the divertor hoop current is decreased at 15 ms

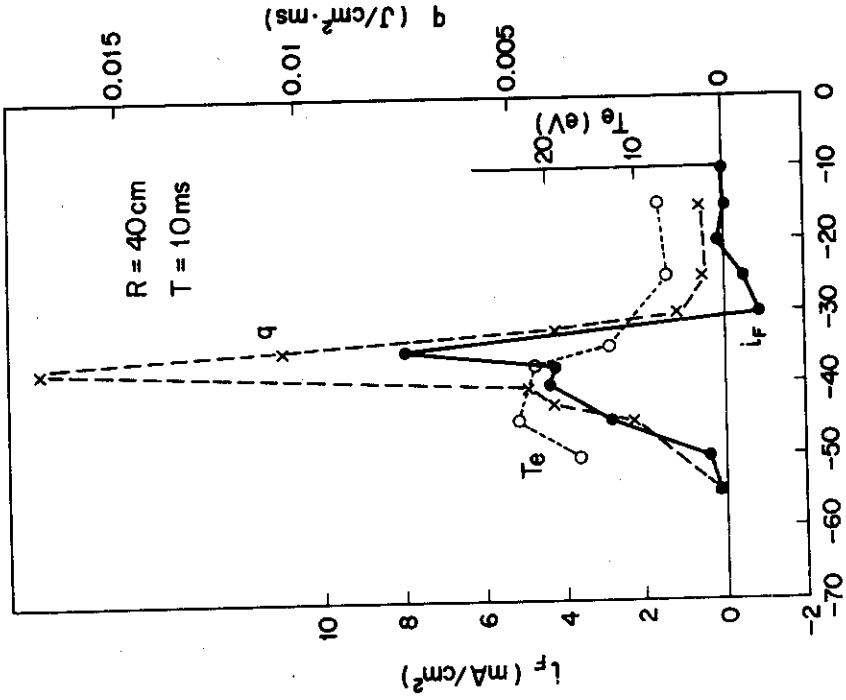

Fig. 20 Profiles of heat flux q(—×—), particles flux i_F (—●—) and electron temperature T_e (—○—)

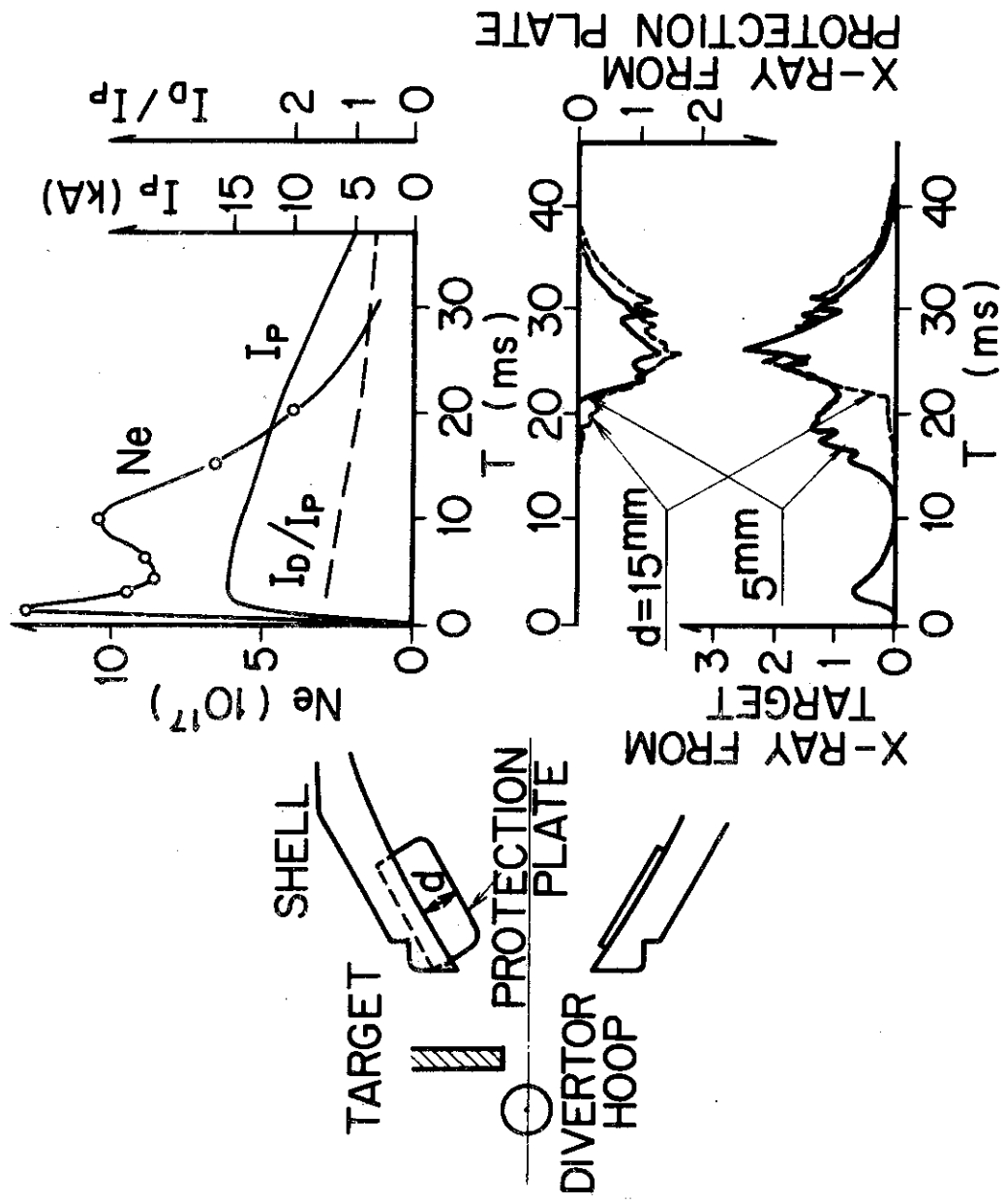

Fig. 22 X-rays from a protection plate and a target

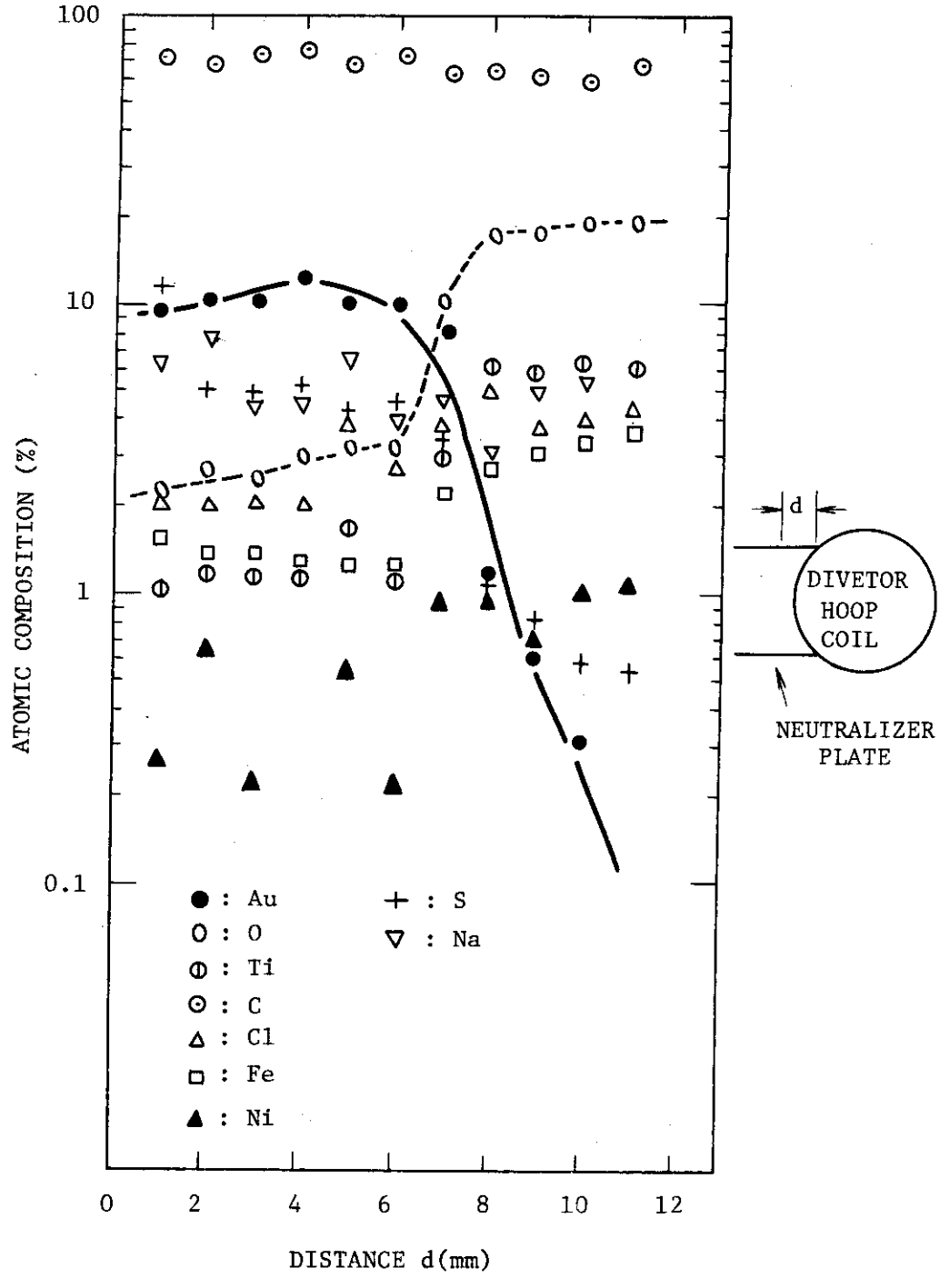

Fig. 23 Surface contamination of the neutralizer plate